Growth Control and Long-Range Self-Assembly of Poly(methyl methacrylate) Nanospheres

Rosaria D'Amato,[1] Iole Venditti,[1] Maria Vittoria Russo,[1] Mauro Falconieri[2]

[1]*Department of Chemistry, University of Rome ''La Sapienza'', p. le A. Moro 5, 00185 Rome, Italy*
[2]*Unità Tecnico Scientifica Materiali e Nuove Tecnologie, Ente perle Nuove tecnologie, Energia e Ambiente (ENEA), C. R. Casaccia, v. Anguillarese 301, 00060 Rome, Italy*

Received 23 March 2006; accepted 26 May 2006
DOI 10.1002/app.24823
Published online in Wiley InterScience (www.interscience.wiley.com).

ABSTRACT: A systematic investigation of the reaction time and role of a cosolvent (toluene) in inducing several beneficial effects on nanobead properties was performed to achieve the synthesis of poly(methyl methacrylate) nanospheres. In particular, good dimensional control in the range of 100–400 nm, very low polydispersity, and a spherical shape were consistently obtained. Different parameters affecting the self-assembly mechanism leading to the deposition of hard-sphere photonic crystals were studied, and the features underlying their role were examined. Photonic crystals were produced by the evaporation of nanosphere suspensions at different temperatures, relative humidities, and suspension ionic strengths and with different substrate materials. The proper conditions for obtaining large crystal domains were determined. © 2006 Wiley Periodicals, Inc. J Appl Polym Sci 102: 4493–4499, 2006

Key words: colloids, emulsion polymerization; self-assembly

INTRODUCTION

The self-assembling behavior of nanosized materials in three-dimensional architectures is a primary goal of science for future applications. In this context, the ordered aggregation of nanoparticles in a proper matrix represents a prerequisite for the achievement of photonic crystals (PCs). PCs are composite materials composed of regularly spaced assemblies of units[1,2] that are able to give rise to Bragg diffraction of ultraviolet, visible, or near-infrared light, depending on the particle array spacing. A large effort is currently devoted to developing chemical approaches that allow the preparation of such materials with mesoscale dimensions.[3,4]

Several materials are used as basic building blocks for assembling ordered systems, including inorganic materials (e.g., silica and titania) and organic materials [e.g., polystyrene (PS) and polyacrylates], the latter having the advantage of greater synthetic flexibility. Among them, poly(methyl methacrylate) (PMMA) and PMMA/PS copolymers are of particular interest because they can be readily synthesized in the form of nanospheres, as reported by Asher et al.,[3] Muller and coworkers,[5–7] and Underwood et al.[8] Besides PC fabrication, another emerging field of application requiring size-controlled, polymeric, submicrometer beads is drug delivery (particularly the immobilization of biological entities on selected carriers).[9,10] In fact, some nanostructured, polymeric particles are suitable material carriers for proteins, cells, and enzymes because of their dimensions and biocompatibility.[11]

The successful preparation of PCs depends on the strict control of the chemical and physical characteristics of the nanospheres and on the implementation of appropriate deposition techniques. In fact, the photonic band structure of the material and thus its interaction with light are determined by the chemical structure and properties of the materials, particle dimensions, and packing order. Low polydispersity is fundamental to obtain a low defect density and long-range ordering for nanospheres, which are necessary to produce good PCs. For example, a recent study[12] on silica nanoparticles concerning the effect of polydispersity on the presence of stacking faults, vacancies, and interstitials in hard-sphere PCs reported that the presence of spheres with different dimensions is responsible for line dislocations propagating in the crystals; moreover, when the polydispersity is high, the quantity of interstitial sites increases dramatically, whereas the vacancy concentration remains relatively constant. The production of accurately size-controlled nanosphere with predictable and reproducible characteristics requires, in turn, the thorough control of the synthesis procedure, conditions, and parameters.

As for the PC deposition conditions, these must be selected to enhance the ordering action arising from

Correspondence to: M. V. Russo (mariavittoria.russo@uniroma1.it).

Contract grant sponsor: Ministero dell'Università e della Ricerca Scientifica e Tecnologica [through project NANOFASI (FISR 2003)].

the particle interactions, which are due to interparticle forces, such as lateral capillary forces, flotation forces, convection forces, and electrostatic forces when the particles are electrically charged.[3] The control of the action of these forces is also important because they influence the crystal domain size and particle orientation[13–17] for nanospheres of different materials (e.g., silica and PS/PMMA/polyacrylate copolymers).

Despite the necessity of detailed and systematic experimental studies on the synthesis and deposition conditions of PMMA-based PCs, only a few publications in the vast literature on PCs address these topics. For example, in a recent report, theoretical simulations concerning the kinetics of particle formation in microemulsions for different materials (Cu, ZnS, silica, etc.) were presented,[18] but adequate experimental support work has not yet appeared.

To gain deeper insight into the mechanisms underlying particle production and self-assembly, in this article we report a systematic investigation of the synthesis of PMMA PCs. First, we studied the kinetics of polymer particle growth under different reaction conditions, and then we prepared PCs under different deposition conditions, that is, the ambient temperature and relative humidity (RH), the ionic strength of the suspension, and the substrate material, to assess their effects on the dimensions of the crystalline domains. Besides routine chemical characterization, particles were characterized with dynamic light scattering (DLS) and scanning electron microscopy (SEM) measurements, whereas the PC domain dimensions were obtained from the analysis of SEM images of the deposited samples.

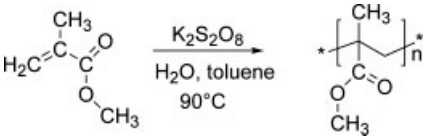

Figure 1 Reaction scheme for the emulsion polymerization of PMMA.

EXPERIMENTAL

Instruments and materials

Deionized water was obtained with a Millipore-Q RG (Milford, CT; CPMQ004R1) and degassed for 30 min with Ar before usage. All the solvents and materials were reagent-grade (Carlo Erba, Milan, Italy); methyl methacrylate (MMA; Aldrich, London, UK; 99% pure) and potassium persulfate (Aldrich; 99.99% pure) were used as received.

Fourier transform infrared spectra were carried out on a PerkinElmer FT 1700X spectrophotometer (Boston, MA) on films obtained via the casting of the aqueous dispersions. ^{1}H- and ^{13}C-NMR spectra were recorded on a Varian Mercury 300 spectrometer (San Francisco, CA) in a $CDCl_3$ solution. The molecular weights were determined by gel permeation chromatography with a PerkinElmer gel permeation chromatography/high-performance liquid chromatography apparatus with an LC250 pump, LC oven, PLgel 10-μm MIX analytical column, an LC 90 J ultraviolet–visible detector, CH_3CN as the eluent, and PS as the standard. The diameter of the beads and their polydispersity were determined with DLS and SEM; the former was particularly useful for obtaining statistically significant measurement of the nanosphere polydispersity. DLS measurements were performed with a Malvern PCS 4800 apparatus on samples diluted in deionized water, and the experimental data were analyzed with the cumulant method to obtain the first (Z-average) and second moments (polydispersity) of the particle distribution function.[19] SEM imaging was carried out with a Leo 1450VP scanning electron microscope (Thomwood, NY) for metalized samples and a Leo 1530 SEM-FEG (scanning electron microscopy-field emission gun) (courtesy of Dr. L. Pilloni, ENEA) for samples deposited on graphite. The dimensions of the crystalline domains were determined from the SEM images of films deposited via casting with an image analysis software tool (Scion Image for Windows, version Beta 4.0.2, Scion Corp., Frederick, MD). We considered domains limited by extended defects (grain boundaries, stacking faults, and dislocations), and cracks were also considered as domain-delineating defects, whereas we did not consider point defects to be domain limits; for each sample, 10 images at about 8000 $\times$ magnification (the best condition for discriminating the domains and their defects) were examined, and then we considered the best measurement results.

PMMA nanobead synthesis

PMMA nanobeads were synthesized with a modified emulsion polymerization in an aqueous dispersion (see Fig. 1); in a typical procedure, 40 mL of deionized water, 14.00 g (0.14 mol) of MMA, and the proper quantity of toluene, used as a cosolvent, were stirred in an Ar atmosphere at 90°C for 2 h. Then, 500 mg of potassium persulfate (10 mL of a 50 g/L degassed solution in deionized water) was added, and the reaction was refluxed under vehement stirring in an Ar atmosphere. The polymerization was stopped by the opening of the flask; the milky white and opalescent emulsion was filtered through a standard paper filter to get rid of large agglomerates and then centrifuged and redispersed with deionized water from two to five times to remove the unreacted monomer and toluene. The reaction kinetics were studied by the withdrawal (10 mL) of the emulsion from the batch reaction by a cannula at fixed times. The molecular weights of the samples, measured by gel permeation chromatography, were as follows: the weight-average molecular weight was 1–5

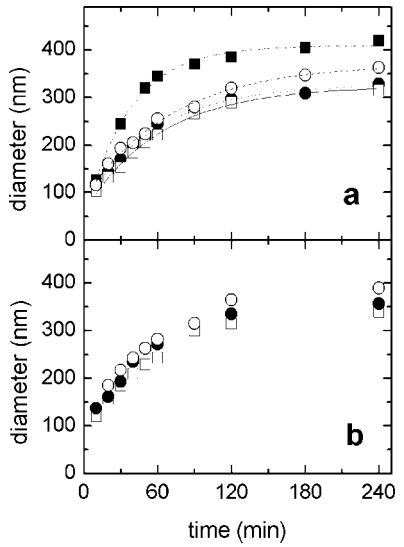

Figure 2 Diameter of the PMMA nanobeads, obtained with (a) SEM and (b) DLS, as a function of the reaction time with different toluene/monomer ratios: (■) 0/1, (□) 1/1, (●) 2/1, and (○) 4/1). The solid line in part a is the fit obtained with eq. (1).

$\times 10^3$ amu, and the weight-average molecular weight/number-average molecular weight ratio was 1.5–1.8.

IR (cm^{-1}): 3000, 2950 (ν_{C-H}); 1735 ($\nu_{C=O}$), 1484, 1380 (δ_{CH}); 1270, 1240, 1191, 1149 (ν_{C-O}). ^{1}H-NMR (δ, ppm): 3.57 (s, 3H, OCH_3), 1.8 (m, 2H, CH_2), 1.18–0.99–0.81 (s, CH_3). ^{13}C-NMR (ppm): 177.8 (CO_2Me), 54.4 (CH_2), 51.8 (OCH_3), 44.9 (C chain), 16.5 (CH_3).

PC deposition

Films of PMMA nanobeads with a diameter of 250 nm were prepared via the casting of a drop of an emulsion onto different substrates under controlled conditions and were characterized with an SEM technique. Depositions of PMMA suspensions at different RH values were performed at room temperature in a climatic chamber in the presence of saturated solutions of different salts [$NaOH \cdot H_2O$, RH = 6%; $KOH \cdot 2H_2O$, RH = 9%; $CaCl_2 \cdot 6H_2O$, RH = 29%; $Ca(NO_3)_2 \cdot 6H_2O$, RH = 51%; NH_4NO_3, RH = 62%; NaCl, RH = 75%; and KCl, RH = 84%]. Depositions at selected temperatures (2–50°C) were made inside a thermostatic chamber at 45–55% RH. Depositions from suspensions with different ionic strengths were carried out at room temperature and humidity with NaCl or $MgSO_4$ solutions at different concentrations, which were added to the emulsion and shaken for 10 min. The different substrates used for the deposition of the polymeric films were cover glass, silica, gold, and graphite.

RESULTS AND DISCUSSION

Synthesis of the PMMA nanospheres

The evolution of the nanobead dimensions during syntheses with different concentrations of the cosolvent toluene was investigated with DLS and SEM as a function of the reaction time in the range of 10–240 min [see Fig. 2(a,b)]. The dimension obtained from the DLS measurements is actually the *Z*-average value, which is the mean diameter weighted over the scattered light intensity, and thus it is not directly comparable with SEM data; however the growth trends of the nanoparticles are similar for the two methods. We can see that in the presence of toluene, the growth rate is slower: the size increases initially from 100 to 250 nm; after 60 min, the growth slows, with final dimensions smaller than 350 nm. The interpretation of this result is based on the assumption that the polymerization without toluene shows a different behavior: the initial growth is faster (350 nm in 60 min), and the final dimension of the particles is larger, up to 420 nm. This behavior is consistent with the study by Tanrisever et al.[20] on PMMA polymerization kinetics: during the first 30 min, the particle growth is due to polymer chain growth; after this time, different polymer chains aggregate each other, and agglomeration and particle coalescence also occur.

To model the kinetics of the particle growth, we fitted the SEM experimental values of the particle dimension as a function of the reaction time with an expression containing parameters useful for the discussion. In particular, we adopted an empirical formula that accurately reproduces our data for the whole range of experimental parameters:

$$d = d_\infty - (d_\infty - d_0)\exp(-t/\tau) \quad (1)$$

Expression (1) describes an exponential growth of the particles, with the time constant equal to τ and the initial ($t = 0$) and final ($t = \infty$) dimensions equal to d_0 and d_∞, respectively. Fits of the experimental data obtained with eq. (1) are reported in Figure 2(a), and the fit parameters are shown in Table I for the different reaction conditions. The presence of toluene clearly increases τ by about a factor of 2. d_0 increases with the toluene volume because in this case the cosolvent drops are bigger and contain a larger quantity of the monomer, this interpretation being in agreement with Lopez-Quintela's work[18] about the synthe-

TABLE I
Best Fitting Parameters Obtained from SEM Experimental Data with Eq. (1)

Toluene/monomer (vol %)	τ (s)	d_∞ (nm)	d_0 (nm)
0/1	36 ± 3	409 ± 6	37 ± 2
1/1	62 ± 4	324 ± 5	59 ± 2
2/1	59 ± 4	328 ± 5	74 ± 3
4/1	72 ± 6	371 ± 8	86 ± 4

sis of microemulsions. The cosolvent forms a layer around the monomer droplets; this layer controls the transfer of monomer molecules from inside the droplets to the surrounding aqueous phase and can absorb the monomer molecules that are dispersed in the solvent. Because of the long-time behavior for the achievement of large nanobeads, this is dominated by coalescence among particles. In the absence of toluene, d_∞ is larger because coalescence occurs among relatively large particles because under this condition τ is short. In the presence of toluene, the size of the drop limits the dimension of the particle and also determines the probability of collision, which is necessary for coalescence, both mechanisms resulting in a moderate increase in d_∞ with the toluene volume fraction, as shown in Table I.

DLS measurements of the samples prepared without toluene gave polydispersity values close to 10^{-1}; however, a small quantity of toluene (e.g., toluene/monomer ratio ≥1) in the synthesis suspension was sufficient to achieve a polydispersity less than or equal to 10^{-2}. The samples were examined also with SEM measurements, which confirmed these outcomes: a high polydispersity and irregular particle shape were found for those samples prepared in the absence of toluene, and very low polydispersity and a regular round shape were found for the other samples (see Fig. 3). These results again point out the role of the cosolvent. In fact, the cosolvent acts as a hydrophobic layer and reduces the potential energy of the interface, leading to an overall stabilization of the emulsion and hence to regularly shaped particles.[16] These results are analogous to the work of Capek[21] on the role of nonionic and ionic/nonionic emulsifiers in the radical polymerization of unsaturated monomers [styrene, alkyl(methacrylates), etc.] in aqueous emulsions; there the increased stability of the emulsions containing a nonionic emulsifier was attributed to the effects produced by the presence of a layer of the emulsifier around the monomer droplets.

A number of experiments were performed to test the reproducibility of the shapes and dimensions of the polymer nanobeads, and the results show that effective control of these parameters in a range useful for PC deposition can be achieved through accurate control of the reaction time and of the concentration of the cosolvent.

The spectroscopic characterization performed on all the synthesized materials gave information about their tacticity according to literature reports.[22,23] IR spectra showed the typical absorption bands of PMMA, particularly in the region of 1300–1100 cm^{-1}, which gives information on the tacticity of PMMA: four high-intensity absorption bands at 1270, 1240, 1192, and 1149 cm^{-1} are typical for a polymer rich in syndiotactic content. ^{1}H-NMR shows the peaks of α-methyl protons of syndiotactic and heterotactic PMMA at 0.81 and 0.99 ppm, respectively, with an intensity ratio of 2/1, and also a less intense peak at 1.18 ppm due to isotactic chain conformation; ^{13}C-NMR spectra present the peak due to C=O_2Me at 177.8, confirming the high percentage of syndiotactic conformation in our samples.

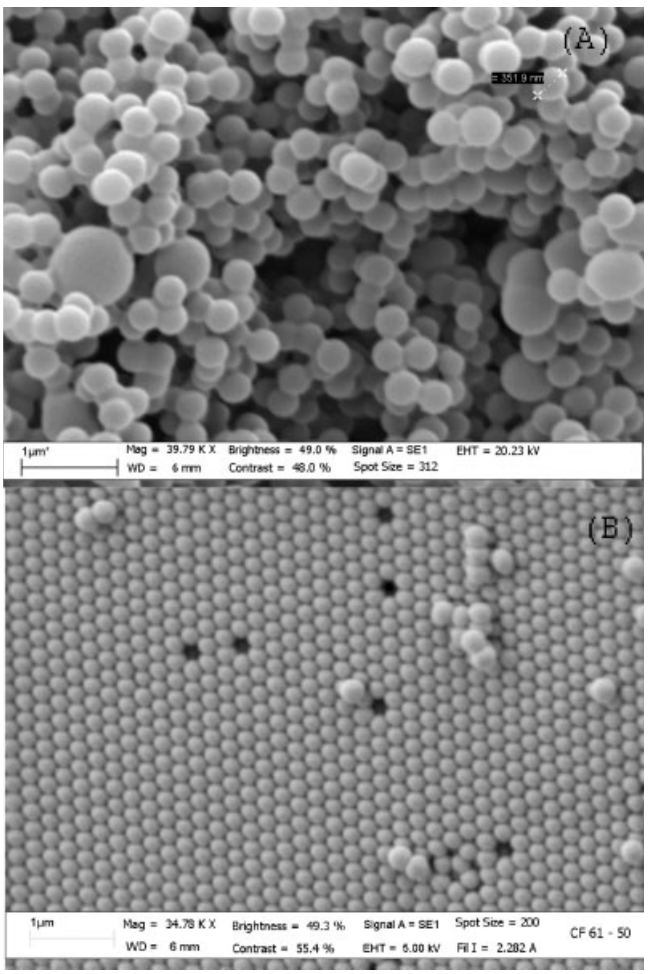

Figure 3 SEM images of PMMA nanobeads obtained under different synthesis conditions: (A) synthesis without toluene (90 min, diameter = 350 nm) and (B) synthesis with 2/1 toluene/MMA (50 min, diameter = 217 nm).

PC deposition

When PCs were deposited under room conditions, the resulting crystals were characterized by relatively large ordered domains, with defects consisting mainly of stacking faults together with some pores associated with missing particles. Our samples presented a brilliant iridescence, an index of the presence and quality of the photonic band gap of the ordered PMMA nanospheres. The three-dimensional ordering was confirmed by the SEM image (Fig. 4). The crystalline structure was determined with the procedure outlined by Koh et al.[24] to be face-centered-cubic. We then investigated the variation of the temperature

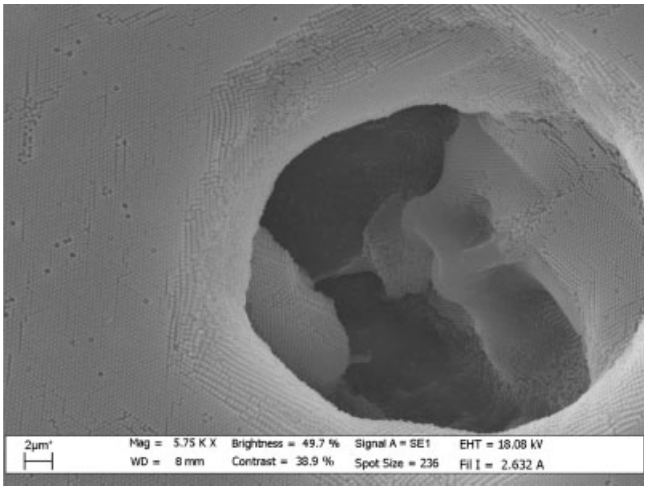

Figure 4 SEM image of three-dimensional ordered domains detectable from an incidental defect of a PMMA nanosphere film.

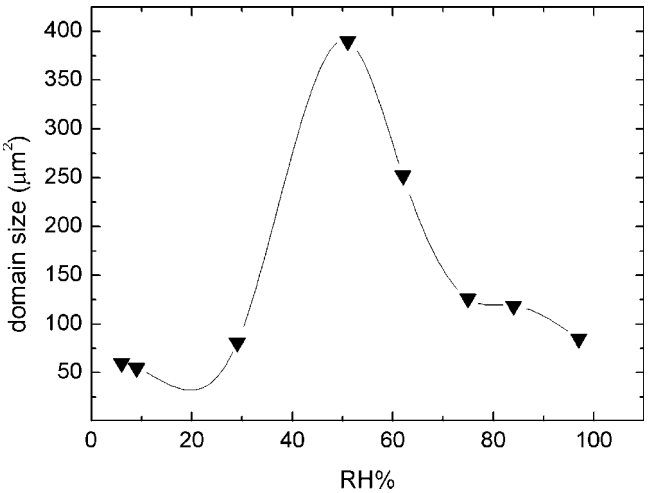

Figure 5 Size of the crystal domains versus RH. The films were obtained via casting at room temperature (the solid line is only a guide to the eye).

and RH to vary the solvent evaporation rate, which has a strong impact on the dynamics of the self-assembly of PMMA suspensions. Besides, the solution ionic strength and substrate material were also varied to study their influence on the PC deposition.

Effect of the evaporation rate

The effect of RH and temperature on the PC domain dimensions is reported in Figures 5 and 6, respectively. Small domains were obtained when the polymer dispersions were dried at low RHs or at high temperatures. Under these conditions, the formation of large ordered arrays is prevented because of the fast evaporation of the solvent, which limits the time allowed for particles to find their minimum energy position. From Figure 5, it is apparent that larger domains are formed at an intermediate evaporation rate, so the probability of introducing defects into the growing crystal is lower under this condition. At an optimum evaporation rate, the particle flux leading to the growing crystals will be sufficiently high to dominate the particle diffusion but slow enough to allow the particle rearrangement and the elimination of defects in crystal sites, as shown also for silica monolayers.[13] The temperature effect, that is the existence of an optimal temperature already investigated,[14] which maximizes the dimensions of domains, is reported for our samples in Figure 6. This effect is clearly understood when we consider that low temperatures freeze the particles, whereas high temperatures enhance the evaporation rate of the solvent, both cases limiting the possibility of finding the minimum energy positions. Temperatures higher than 50°C could not be used because of softening of the polymer beads.

Experimentally, the largest domain size of 390 μm^2, corresponding to a minimum density of extended defects, was obtained under intermediate deposition conditions (RH = 50% and temperature = 25°C).

Effect of the ionic strength

The intensity of the particle interactions arising from electrostatic and capillary forces can be modulated by the variation of the electrolyte concentration inside the suspension. The addition of salts has been shown[13–16] to reduce the electrostatic screening length, leading to a exponential reduction of the crystalline domain dimensions in silica PCs. We systematically changed the ionic strength of the suspension by adding NaCl or $MgSO_4$, and we characterized the domain dimensions as previously described. Because a high salt concentration causes

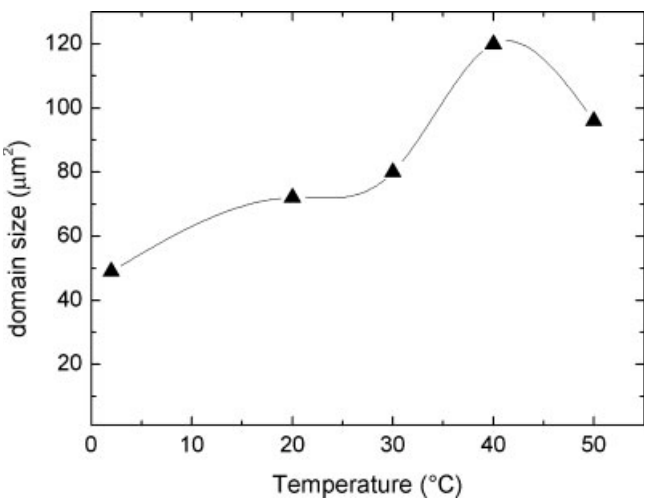

Figure 6 Size of the crystal domains versus the temperature. The films were obtained via casting at 30–60% RH (the solid line is only a guide to the eye).

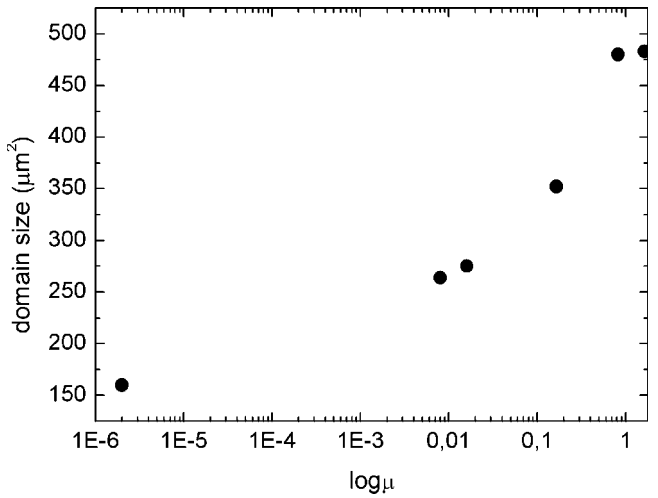

Figure 7 Size of the crystal domains versus the ionic strength (μ) of the suspension. The films were obtained via casting at room temperature and 30–60% RH.

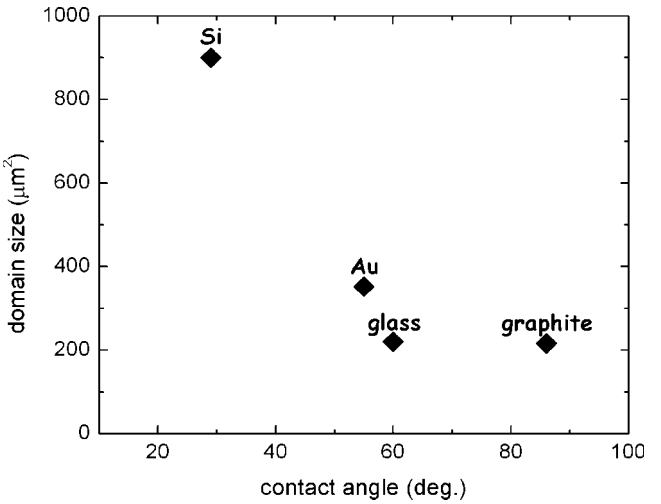

Figure 8 Size of the crystal domains as a function of the suspension–substrate contact angle as produced by deposition on different substrates at room temperature and 30–60% RH.

salt precipitation, which is deleterious for PC formation,[12,13] we used $MgSO_4$ to obtain a higher ionic strength with a smaller amount of salt in comparison with NaCl. Figure 7 shows the relationship between the ionic strength of the PMMA suspensions and the obtained crystal domains. Under our experimental conditions the domain dimensions increase with the ionic strength of the suspension. This behavior is different from that reported in the literature for silica PCs; however, it is not clear whether in that case PC formation was limited by salt precipitation.[13–16] With NaCl, in most cases salt cocrystallization occurred, and only in salt-free areas of the film there were small ordered domains. Moreover, cocrystallization prevented an accurate study of the domain dimensions.

In general, a trend can be outlined: an increase in the ionic strength of the PMMA suspension improves the domain dimension and the quality of the PCs. The addition of electrolytes induces changes in the colloidal stability and in the particle interaction during the drying procedures. With increasing ionic strength, crystal domains rapidly assemble because the electrostatic repulsion among polymer particles and between the polymer particles and substrate are reduced, and an increase in the Brownian motion of the particles occurs, so they easily adopt their lowest free energy configuration. However, at a high salt concentration, the coprecipitation of salt affects the system, and long-range order is suppressed. These results point out the importance of capillary forces in assisting the ordered deposition of PCs[24] versus electrostatic forces, as discussed in the next section.

Effect of the substrate

The substrate suitability for polymer PC deposition from aqueous suspensions is mainly related to its wettability because this property influences essentially the liquid–solid interface region in which the capillary forces are dominant. Obviously, a good substrate must possess other characteristics as well, such as low roughness and good chemical affinity for the polymer material.

To explore the substrate effect on the PC quality, we chose to cast films of PMMA on different substrates representative of important classes of materials (e.g., oxides, semiconductors, and metals) and of different areas of applications, from optical devices to electronics. In particular, we selected a cover glass, graphite, gold, and silicon. A recent work[24] on the deposition of polymeric PCs onto silicon and aluminum substrates showed that, to exploit the ordering action of capillary forces, a low contact angle is desirable. Our experimen-

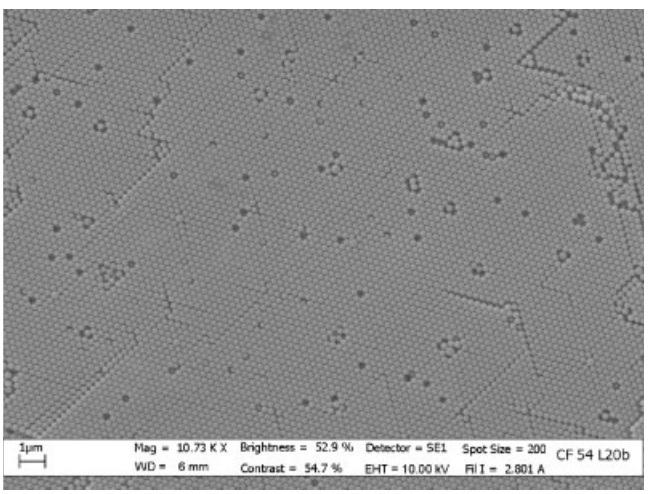

Figure 9 SEM image of a film of PMMA deposited on Si at 25°C and 30–60% RH. The crystal domain size is 900 μm².

tal evidence confirms this mechanism, as shown in Figure 8. In fact, larger ordered domains were detected on wettable surfaces, evidencing an inverse relationship between the contact angle and the size of the ordered domains. A possible explanation is related to the thinner meniscus region, which limits the number of colloids layers: thinner colloidal crystals can cover larger areas with few extended defects. Thus, an accurate selection of substrate material can substantially improve the PC quality. As a matter of fact, the largest crystal domains of about 900 μm^2 were obtained after deposition on the silicon substrate (Fig. 9).

CONCLUSIONS

A systematic study of the particle growth, depending on the reaction time and cosolvent volume in the emulsion polymerization of PMMA nanoparticles, was performed, and the nanosphere dimensions were characterized with SEM and DLS. In particular, the use of a cosolvent was shown to increase the time constant of the reaction, giving the possibility of more precise control of the diameter of the particles. Furthermore, in the presence of the cosolvent, a very low polydispersity and spherical particle shape were obtained, both conditions being of the utmost importance for the deposition of quality PCs.

The proper conditions for PC deposition were investigated by changes in the temperature, RH, suspension ionic strength, and substrate material. A wettable substrate material, together with intermediate values of the temperature and RH, led to optimization of the domain size. Unlike previous reports, a high ionic strength was shown to be beneficial for quality PC depositions. We obtained the largest crystalline domains (900 μm^2) by the deposition of PMMA nanobeads on a silicon substrate at room temperature and 50% RH.

The authors thank L. Pilloni (ENEA) and D. Ferro (University of Rome ''La Sapienza'') for the scanning electron microscopy imaging.

References

1. Yablonovitch, E. Phys Rev Lett 1987, 58, 2059.
2. John, S. Phys Rev Lett 1987, 58, 2486.
3. Reese, C. E.; Guerrero, C. D.; Weissman, J. M.; Lee, K.; Asher, S. A. J Colloid Interface Sci 2000, 232, 76.
4. D'Amato, R.; Medei, L.; Venditti, I.; Russo, M. V.; Falconieri, M. Mater Sci Eng C 2003, 23, 861.
5. Muller, M.; Zentel, R.; Maka, T.; Romanov, S. G.; Torres, C. M. S. Chem Mater 2000, 12, 2508.
6. Muller, M.; Zentel, R.; Maka, T.; Romanov, S. G.; Torres, C. M. S. Adv Mater 2000, 12, 1499.
7. Romanov, S. G.; Maka, T.; Torres, C. M. S.; Muller, M.; Zentel, R. Synth Met 2001, 124, 131.
8. Underwood, S. M.; Van Megen, W.; Pusey, P. N. Phys A 1995, 221, 438.
9. Choi, S. K.; Kim, D. J Appl Polym Sci 2002, 83, 435.
10. Ge, H.; Hu, Y.; Yang, S.; Jiang, X.; Yang, C. J Appl Polym Sci 2000, 75, 874.
11. Panzavolta, F.; Soro, S.; D'Amato, R.; Palocci, C.; Cernia, E.; Russo, M. V. J Mol Catal B 2005, 32, 67.
12. Pronk, S.; Frenkel, D. J Chem Phys 2004, 120, 6764.
13. Rödner, S. C.; Wedin, P.; Bergstrom, L. Langmuir 2002, 18, 9327.
14. Cong, H.; Cao, W. Langmuir 2003, 19, 8177.
15. Bevan, M. A.; Lewis, J. A.; Braun, P. V.; Wiltzius, P. Langmuir 2004, 20, 45.
16. He, C.; Donald, A. M. Langmuir 1996, 12, 6250.
17. Rakers, S.; Chi, L. F.; Fuchs, H. Langmuir 1997, 13, 7121.
18. Lopez-Quintela, M. A. Curr Opin Colloid Interfaces Sci 2003, 8, 137.
19. Koppel, D. E. J Chem Phys 1972, 57, 4814.
20. Tanrisever, T.; Okay, O.; Sonmezoglu, I. C. J Appl Polym Sci 1996, 61, 485.
21. Capek, I. Adv Colloid Interfaces Sci 2002, 99, 77.
22. Grohens, Y.; Proud'homme, R. E.; Schultz, J. Macromolecules 1998, 31, 2545.
23. Jiang, W.; Yang, W.; Zeng, X.; Fu, S. J Polym Sci Part A: Polym Chem 2004, 42, 733.
24. Koh, Y. K.; Teh, L. K.; Wong, C. C. Communication to Advanced Materials for Micro- and Nano-Systems, Singapore, 19–20 January, 2005.